Title

Charge Distribution on S and Intercluster Bond Evolution in Mo6S8 during the Electrochemical Insertion of Small Cations Studied by X-ray Absorption Spectroscopy

Journal

The Journal of Physical Chemistry Letters, 10(6)

ISSN

1948-7185

Authors

Yu, Pengfei

Long, Xinghui

Zhang, Nian

et al.

Publication Date

2019-03-21

DOI

10.1021/acs.jpclett.8b03622

Peer reviewed

Charge distribution on S and intercluster bond evolution in Mo_6S_8 during the electrochemical insertion of small cations studied by X-ray absorption spectroscopy

Pengfei Yu[†]*, Xinghui Long[†], Nian Zhang[†], Xuefei Feng[§], Jiamin Fu[†⊥], Shun Zheng[†], Guoxi Ren[†], Xiaosong Liu[†⊥]*, Cheng Wang[§], Zhi Liu[†⊥]

[†] State Key Laboratory of Functional Materials for Informatics, Shanghai Institute of Microsystem and Information Technology, Chinese Academy of Sciences, 200050, China

[§] Advanced Light Source, Lawrence Berkeley National Laboratory, Berkeley, California 94720, United States

[⊥]School of Physical Science and Technology, Shanghai Tech University, Shanghai 200031, China

KEYWORDS: X-ray absorption, rechargeable magnesium batteries, Chevrel phases, charge distribution, bond evolution

ABSTRACT: Chevrel phase Mo_6S_8 has aroused special interest as promising cathode material in rechargeable Mg batteries since 2000. Despite extensive studies on the mechanism of cation accommodation, some fundamental questions are still unclarified, including but not limited to the origination of the chemical stability, key factors inducing the structural evolution and the factors related to the electrochemical reversibility. Here, the Mo $L_{2,3}$ and S K-edge X-ray absorption spectroscopy were utilized to study the charge distribution on S and intercluster bond evolution in Mo_6S_8 during the cation insertion. S K pre-edge features can be assigned to two kinds of S with different nuclear effective charge by the 2nd derivatives, indicating the non-uniform charge distribution on S. With one cation inserted, the disappearance of the feature of S K-edge centered around 2468.1 eV indicates the charge distribution on S becomes homogeneous, which is related to the chemical stability and electrochemical reversibility. The evolution of certain Mo $L_{2,3}$ and S K pre-edge features with the insertion of different types of cations indicates that the structural evolution should result from the change of bond length induced by delocalization of inserted cations, which gives a support to the “matrix effect”. Moreover, drastic change of the intensity of S K pre-edge centered around 2469.4 eV mainly results from the evolution of intercluster Mo-Mo bond length, which is closely related to the electrochemical reversibility. We hope this study sheds light on the afore-mentioned questions and guides the rational design of Mg cathode material.

INTRODUCTION

Chevrel phases Mo_6T_8 (T=S, Se, Te), where the Mo_6-octahedral clusters inside T_8 cubes are linked by Mo-Mo and Mo-T bonds to form a three-dimensional network, can accommodate almost 40 varieties of cations to form $M^{n+}{}_xMo_6T_8$. According to the size of cation M, a rough classification was proposed: type I, Chevrel phases with one large cation (> 1 Å, M = Pb, Sn and rare-earth metal, etc.) occupied the center of the largest cavity, and type II, Chevrel phases with small cations (< 1 Å, M = Li, Cu, Na, etc.) inserted where the maximal amount was thought to be limited by the accommodation capability of accompanied electron. Type I was studied widely because of its superior superconductive properties such as high superconductive transition temperatures and high critical fields.[1-7] However, type II was comparatively less studied although it could be used for electrochemical energy storage owing to the novel mobility of cation M under electromotive force. [8-14]

Until 2000, the excellent performance of Mo_6S_8 as a cathode in rechargeable Mg batteries reported by Aurbach et.al[15] triggered great interest on insertion of small cations into Chevrel phases.[16-21] From then on, many theoretical[22-27] and experimental studies from the point view of electrochemistry[18, 28-30] and structure[31-36] have been performed to illustrate the reaction mechanism. However, the fact that Chevrel phases are still the unique reversible cathodes up

to now reminds us many fundamental issues still need to be clarified.

One of the main debates lies in structural evolution with the insertion of cations ranging in charge and radius. Yvon demonstrated for the first time that the charge and concentration of cations were the only two factors determining the size and distortion of Mo_6 cluster due to the charge transfer from cation to Mo_6 cluster.[37] They proposed "cluster valence electron concentration" (cluster-VEC) to evaluate the effect of charge transfer on the distortion of Mo_6 octahedron along with the insertion of cations. With the cluster-VEC close to the theoretical maximum 24, the shape of the Mo_6 octahedron became much more regular, leading a structural stability.[37-39] By virtue of this model, we could understand why pure Mo_6S_8 (cluster-VEC = 20) could only be prepared by chemical or electrochemical corrosion while $Mo_6S_6I_2$ and $Mo_6S_6Br_2$ (cluster-VEC = 23.67) could be synthesized directly. However, the model was not able to explain some other cases. For cations like Li^+, Na^+, Mg^{2+}, and so forth, the Chevrel phases with nx = 1 or 2 (cluster-VEC = 21 or 22) could be obtained relatively easily by the direct high-temperature-synthesis, but compounds with nx = 4 (cluster-VEC = 24) could only be prepared by cation insertion chemically or electrochemically.[36] Moreover, electrochemical studies[12, 40] revealed that cation insertion with nx up to 4 was possible for both the Mo_6Se_8 (cluster-VEC = 21) and Mo_6Te_8 (cluster-VEC = 22), exceeding the theoretical maximum 24 of the model.

The cluster-VEC model was criticized by Corbett.[41] Instead, he proposed the key role of "matrix effect" on the Mo_6-cluster shape. More specifically speaking, cation insertion could decrease repulsive interaction between the anion closed shells associated by a loosening of Mo-T intercluster bonds and thus lead to the decrease of Mo_6 elongation. In his study, the pauling strength, which is the cornerstone of the modern bond valence (BV) model, was used to compare the metal-metal bonds for Chevrel phases and other similar compounds. A more systematical BV analysis on Chevrel phases was performed by Levi and Aurbach.[42] They argued the intrinsic instability of the binary Chevrel phases did not result from the Mo_6-cluster anisotropy, but rather from the severe non-uniform charge distribution on anions. The charge distribution on anions changed drastically with cation insertion, leading to the structural stabilization. However, all the conclusions obtained by Corbett and Aurbach were theoretical prediction based on BV model. Direct experimental evidence is still lacking. Although Kubel and Yvon[43] once made a study on "matrix effect", it mainly focused on large cations (> 1 Å) but not on small cations inserted electrochemically.

X-ray absorption spectroscopy (XAS) is one of the most powerful methods to provide insight into the electronic structure of selected absorbing atoms. In particular, transition metal L-edge and ligand K-edge XAS can give detailed information on unoccupied states right near the Fermi level, such as ligand field, spin states and hybridization, which are the key factors to regulate the fundamental properties and practical performances of materials. The information on chemical bonds can also be obtained as the chemical bonds are actually the interaction between the electrons near the Fermi level. Therefore, the transition metal L-edge and ligand K-edge XAS have made their wide application in studying lithium/sodium ion batteries.[44-49] The technique has already been applied to study Chevrel phase as Mg cathode.[50] However, deep discussion on the above debates has not been involved.

In this work, we will study the charge distribution on anions and intercluster bond evolution in a typical Chevrel phase Mo_6S_8 with the insertion of cation in different radius and charge (i.e. Li^+, Mg^{2+} and Cu^+) or in different amount. This study aims to weigh the role of charge effect and "matrix effect" in structural evolution in electrochemical process, provide a direct experimental evidence for charge distribution on anions and intercluster bond evolution during cation insertion, and discuss their relationship with electrochemical reversibility. This study will shed light on the mechanism of Mg storage in Mo_6S_8 and help to guide the development of reversible Mg cathode material.

EXPERIMENTAL

Battery test and sample preparation

Mo_6S_8 and $CuMo_6S_8$ chevrel phases were synthesized firstly according to the previous report. [16] The corresponding XRD patterns and SEM images are shown in Figure S1. The cathode was composed of Mo_6S_8, carbon black (AB) and polyvinylidene difluoride (PVDF) in the weight ratio of 8: 1: 1. Solution of 0.25 M $Mg(AlCl_2BuEt)_2$ in anhydrous THF was used as the electrolyte for Mg batteries. The electrochemical window was tested by CV as shown in Figure S2. The electrolyte for the Li^+ insertion comprised 1mol/L $LiClO_4$ mixed in ethylene carbonate (EC)/diethyl carbonate (DMC) in the volume ratio of 1: 1. The half-cells were assembled with the corresponding pure Li or Mg sheet as anodes. All the operations were done in a pure Ar-filled glovebox with O_2 and H_2O content lower than 0.1 ppm.

All the cells were tested by using the Arbin battery test system. The cells were discharged or charged at the rate of 0.1 C to certain voltage or for certain time to obtain cathodes with specific

amount of cations inserted. Typical discharge/charge profiles are shown in Figure S3. When the tests finished, the cells were transported to Ar-filled glovebox and disassembled at Ar atmosphere. The cathode samples were washed for three times by using anhydrous DMC or THF to decrease the interference from electrolyte. To avoid any possible interference from atmosphere during transportation to Taiwan Light source (TLS), the samples were sealed in aluminium-plastic bags.

Tender X-ray absorption spectroscopy

Sulfur K- and Mo $L_{2,3}$-edge XAS were collected on beamline 16A1 at the TLS in Hsinchu. The solid reference samples (MoS_2 and $MoS_3{\cdot}2H_2O$) were brushed on S-free Kapton tape. All the samples were mounted to a sample holder in a dry glovebox with inert atmosphere (N_2). A 6 μm thick, sulfur-free mylar film was used as front window to prevent the exposure to air when transferring air-sensitive samples from glovebox to test chamber despite that the whole exposure time was no more than 20 s. The sample holder was placed in front of the X-ray beam at a 45° angle. Before collecting data, the chamber was purged with He at least for 30 min. Spectra were collected in bulk sensitive fluorescence yield mode by using a Lytle detector. The photon energy was calibrated with the maximum in the 1st derivative at the L_3-edge of pure Mo foil set to 2520 eV. Background subtraction and normalization were performed by using the Athena software program.[51]

RESULTS AND DISCUSSIONS

The contribution from Mo-Mo bonds

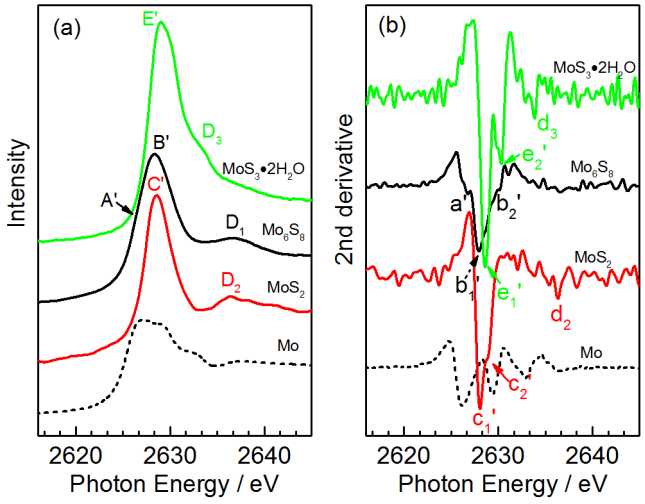

Figure 1. (a) Mo L_2-edge spectra and (b) the corresponding 2nd derivatives of references including $MoS_3{\cdot}2H_2O$, Mo_6S_8 and MoS_2.

The Mo L-edge of $MoS_3{\cdot}2H_2O$, Mo_6S_8 and MoS_2, which further splits into L_2 and L_3-edge because of the 2p core-hole spin-orbital coupling, were firstly studied. It has been reported that the multiplet effect is so small for the $L_{2,3}$-edge of 4d elements that the intensity ratio between L_3 and L_2-edge is closed to 2:1 (see the details of Mo L-edge in Figure S4).[52, 53] Moreover, the L_2 edge has been thought to be more related to the single-particle model due to the less weight of intensity transfer between peaks at L_2-edge than that at L_3-edge.[52, 53] In addition, Mo L_2-edge is also less interfered by the S K-edge than L_3-edge, which makes the normalization more correctly. Therefore, Mo L_2-edge are mainly used for comparison in Figure 1 (a) while L_3-edge can be found in Figure S5. Generally, each L_2-edge has two obvious features, which are marked as C' and D_2 for MoS_2, B' and D_1 for Mo_6S_8 and E' and D_3 for $MoS_3{\cdot}2H_2O$, respectively. The peaks D_1, D_2, and D_3 lie above the ionization potential and have been assigned to the multiple scattering resonance[54] or transition to quasi-bound states[55]. Peak B', C' and E' are assigned to the transition from $2p_{1/2}$ to 4d states, which will be focused in our study. The energy position of B' is a bit lower than C', while much lower than E'. One of the main contributions to the peak position comes from the effective charge of transition metal. Thus, it might indicate the effective charge of Mo in Mo_6S_8 is very close to that in MoS_2 while smaller than that in $MoS_3{\cdot}2H_2O$ though the peak position was more or less impacted by ligand field.[56, 57] It can be well supported by the comparison of spectra of Mo K-edge as shown in Figure S6. Besides, the profile of peak B' is a bit broader than the peak C'. The detailed difference in profile between B', C' and E' can be found according to the 2nd derivatives in Figure 1(b). As the peak valley of the 2nd derivatives represents the peak position and can be used to distinguish the refined features in the spectrum, it reveals the L_2-edge of Mo_6S_8 contains three peaks (a', b_1' and b_2') while the peak C' can be divided into two peaks marked as c_1' and c_2'. Moreover, the peak intensity (the absolute value) of a', b_1' and b_2' are much lower than that of c_1' and c_2' and that of e_1' and e_2' for $MoS_3{\cdot}2H_2O$ overall. The intensity of peak valley can tell the curvature of the corresponding XAS feature, mainly related to the peak width if not much intensity change of the XAS feature. Therefore, the obvious lower peak intensity indicates the broader peak width of the XAS features of Mo_6S_8. As the peak width is thought to be related to the width of energy bands, it indicates that the energy bands in Mo_6S_8 are generally broader than those of the other two. The broadening of energy bands of Mo_6S_8 should consist of the contribution from Mo-Mo bonds, which has been predicted in theoretical studies.[3, 6]

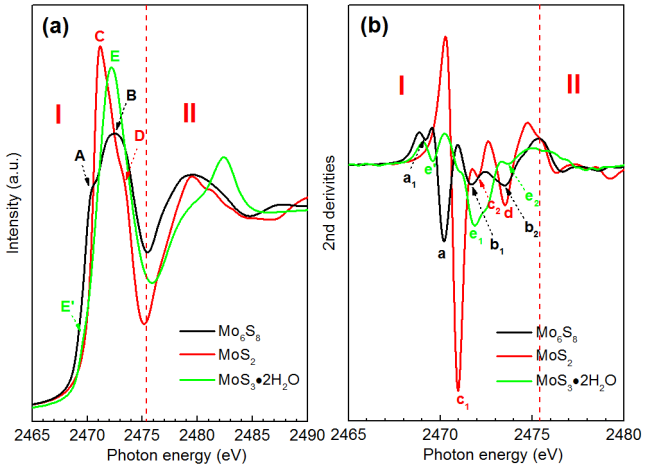

Figure 2. (a) The S K-edge X-ray absorption spectra of MoS_2, Mo_6S_8 and $MoS_3{\cdot}2H_2O$, as well as (b) the 2nd derivatives of these spectra.

S K-edge X-ray absorption spectra of MoS_2, Mo_6S_8 and $MoS_3{\cdot}2H_2O$ are studied to get information on metal-ligand bonding interactions more directly. As shown in Figure 2 (a), the spectra can be generally divided into two regions despite a large overlap between them: the sharp "pre-edge" features below 2475 eV marked as I, and the broad humps at higher energy marked as II. The region I originates from electron transitions from ligand 1s core levels to the partially filled Mo 4d states hybridized with S 3p states. The region II results from the transitions to bound states (including 4p states) with higher energy than the ionization.[57, 58]

The pre-edge peaks of the three sulfides have high intensity, indicating a high covalency of the Mo-S bond. In other words, there is high hybridization between Mo and S in the three compounds. Moreover, the pre-edge peak of Mo_6S_8 is broader than those of MoS_2 and $MoS_3{\cdot}2H_2O$. The trend is the same as that at Mo L_2-edge, indicating the dominating role of Mo 4d bands in the LUMO. More details of pre-edge can be obtained according to the 2nd derivatives, which has been proved to be a useful way in spectrum studies on S K-edge.[59-61] As shown in Figure 2 (b), the pre-edge of Mo_6S_8 contains 4 refined peaks (a_1, a, b_1, b_2) in the range of 4 eV, while 3 peaks for MoS_2 in the range of 2.6 eV and 3 peaks for $MoS_3{\cdot}2H_2O$ in the range of 3 eV, respectively.

Charge distribution

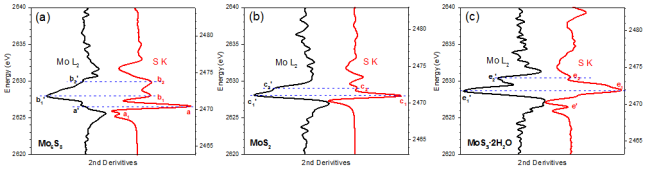

Figure 3. Alignments of 2nd derivatives of S K with Mo L_2 pre-edge features for (a) MoS_2. (b) Mo_6S_8, (c) $MoS_3{\cdot}2H_2O$, respectively.

Because of the decisive role of Mo 4d bands on the S K pre-edge while the notable reduction of multiplet effect on Mo L_2-edge,[53, 62] Mo L_2-edge is thought to correspond more explicitly to S pre-edge. Such correlations can be further confirmed by the alignments of 2nd derivatives of the Mo L_2-edge with those of the corresponding S K pre-edge for Mo_6S_8, MoS_2 and $MoS_3{\cdot}2H_2O$ in Figure 3 (a), (b) and (c), respectively. For Mo_6S_8, all the refined S K pre-edge features except a_1 at lower energy correspond to different features at Mo L_2-edge well. It indicates the origination of a_1 is different from the others. As Mo_6S_8 is conductive, peak a_1 is assigned to the transition from a more shallow 1s core level to the delocalized unoccupied states than the other three. The more shallow S 1s core level results from less effective nuclear charge (Z_{eff}), indicating at least two kinds of S with different Z_{eff} in Mo_6S_8. It is in agreement with the viewpoint from crystal structure. There are two kinds of S existing in Mo_6S_8, where two S_A on the ternary axis are respectively coordinated with 3 Mo atoms while six peripheral S_B are coordinated with 4 Mo atoms, respectively. Moreover, the peak a_1 is assigned to S_A and thus more electrons stay around S_A because the low intensity of peak a_1 can be understood by the less amount of S_A and lower Mo coordination. Our conclusion is in agreement with the previous theoretical calculation.[50] The increase of the local valence electrons on ligand with less cation coordination has already been reported in the other previous XAS study.[63] On the contrary, the electron concentration on S_A has been reported to be lower by using the BV analysis.[42] Therefore, more discussions on the charge distribution are needed. Nevertheless, our result is the first experimental evidence on the non-uniform charge distribution on S in Mo_6S_8. The reliability of our analysis can be further confirmed by the case of $MoS_3{\cdot}2H_2O$. The 2nd derivatives of S K-edge of $MoS_3{\cdot}2H_2O$ in Figure 3(c) also has a small peak e' at lower energy which cannot match with the features of the Mo L_2-edge. If our analysis were reliable, the feature e' should demonstrate there were also two kinds of S in $MoS_3{\cdot}2H_2O$. Actually, it has been demonstrated by XPS and Mo K EXAFS that the formulation of MoS_3 can be written as $Mo^{V}(S_2^{2-})_{1/2}(S^{2-})_2$. [64, 65]

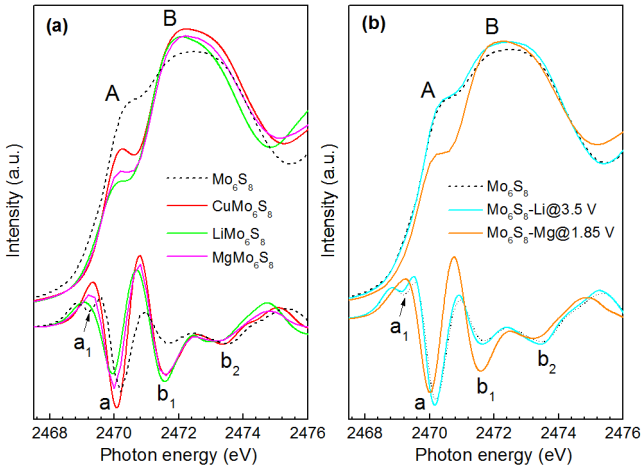

Figure 4. (a) The absorption spectra and the corresponding 2nd derivatives of S K-edge for $CuMo_6S_8$, $LiMo_6S_8$ and $MgMo_6S_8$, (b) the absorption spectra and the corresponding 2nd derivatives of S K-edge for Mo_6S_8 charged to 3.5 V vs. (Li/Li^+) and Mo_6S_8 charged to 1.8 V vs. (Mg/Mg^{2+}). The data of original Mo_6S_8 shown in short dash line is used for comparison.

The charge distribution during cation insertion was further studied by monitoring the evolution of peak a_1. As shown in Figure 4(a), peak a_1 disappears with one Cu^+, Li^+ or Mg^{2+} inserted into Mo_6S_8. According to the discussion above, the absence of peak a_1 indicates that all the S atoms stay in similar environment and own similar Z_{eff}, indicating the homogeneous charge distribution on S. The similar coordinated environment might result from the interaction between S_A and the inserted cations. According to the previous BV analysis, the homogeneous charge distribution on anions can be fulfilled with the entrance of the first two electrons.[42] Our results provide the first direct experimental evidence with more details, where the charge distribution becomes homogenous only with the entrance of one electron. Furthermore, the uneven charge distribution on S has been argued to be the origin of chemical instability of Mo_6S_8.[42] If the conclusion is reliable, our result could give an explanation on the experimental fact that some Chevrel phases with nx = 1 can be obtained relatively easily by the direct high-temperature-synthesis.[36]

The evolution of charge distribution was further checked during electrochemical extraction process. As shown in Figure 4(b), when charged to 1.85 V vs. Mg/Mg^{2+}, peak a_1 cannot re-appear. It is known that 0.5 Mg^{2+} were still trapped. However, when charged to 3.5 V in lithium ion batteries, where all Li^+ were extracted reversibly, peak a_1 is able to re-appear. It tells charge distribution becomes non-uniform with the extraction of the last Li^+. Thus, the electrochemical reversibility corresponds well to the reversible evolution of charge distribution. Given that the chemical stability decreases with a more non-uniform charge distribution,[42] we can conclude that electrochemical reversibility is not only related to chemical stability but also other factors.

The correlation between bond evolution and electronic structure

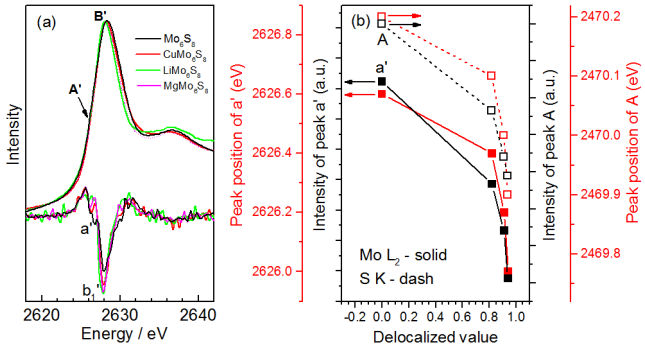

Figure 5. (a) The absorption spectra and the corresponding 2nd derivatives of Mo L_2-edge for Mo_6S_8, $CuMo_6S_8$, $LiMo_6S_8$ and $MgMo_6S_8$, and (b) energy shift and intensity evolution of peak a at Mo L_2-edge and peak A at S K-edge with cation delocalization.

Another obvious change with Cu^+, Li^+ and Mg^{2+} insertion or extraction involved the intensity and energy position of peak A. The evolution of peak A of S K-edge (in Figure 4(a)) as well as the corresponding peak A' of Mo L_2-edge was studied. Figure 5 (a) shows the spectrum and the corresponding 2nd derivatives of Mo L_2-edge. The evolution of peak A' can be distinguished only by the 2nd derivatives. It reveals that the position of peak A (a) and a' shifts to lower energy while the intensity of peak A and a' (the absolute value) decreases with the insertion of Cu^+, Mg^{2+} and Li^+ in sequence, which are not proportional to the amount of charge transfer. The inserted small ions have been reported to delocalize from the center of the inner site, leading a structural distortion. The values of delocalization have been reported: 0.94 for $LiMo_6S_8$, 0.91 for $MgMo_6S_8$ and 0.82 for $CuMo_6S_8$.[66] The correlation between the evolution of peak A and a' and delocalization values are revealed in Figure 5(b). The intensity decreases while position shifts to lower energy with the increase of the cation delocalization. As the pre-edge features are closely related to the Mo-Mo and Mo-S bond, it indicates that the delocalization of the inserted cations is the main cause of the bond evolution, i.e. changes of local structure. In other words, the deformation of Mo_6S_8 should result from the change of bond length induced by delocalization of inserted cations but not from the stabilization of the bonding states through gradual filling of electrons. This gives a support to the "matrix effect".

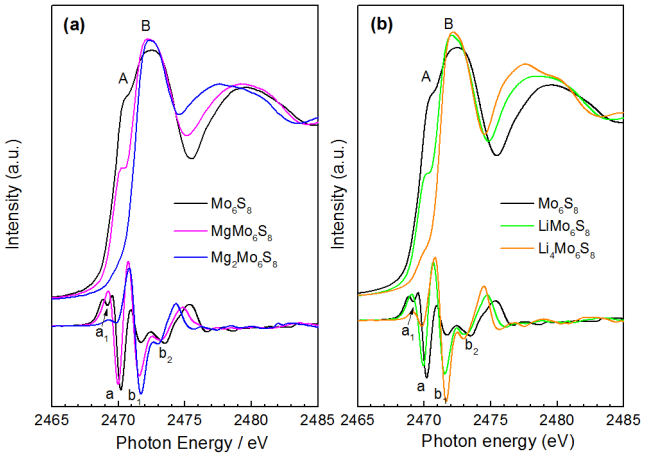

Figure 6. S K-edge X-ray absorption spectra and their corresponding 2nd derivatives for (a) Mo_6S_8, $MgMo_6S_8$ and $Mg_2Mo_6S_8$, and (b) Mo_6S_8, $LiMo_6S_8$ and $Li_4Mo_6S_8$

The correlation between the spectrum and bond evolution during the electrochemical reaction was further studied. As shown in Figure 6(a), with one Mg^{2+} inserted, the intensity of peak A decreases

by nearly 50%; with two Mg^{2+} inserted, it almost disappears. The intensity of the pre-edge peak of S K-edge is mainly affected by the dipole integral of transition from 1s to 3p states, Mo-S covalency and number of hole in the corresponding Mo_6 energy bands.[57, 58, 61, 63] Due to the invariable number of S atoms per Mo_6S_8 unit and the small decrement of the dipole integral from 1s to 3p transition (less than 10% according to ref.[67]) with each Mg^{2+} inserted, the nearly 50% decrement of intensity is thought to result from the Mo-S convalency and the number of holes in specific energy bands. Considering the dominant role of "matrix effect", the covalency could be influenced by Mo-S bond length while the hole number in specific Mo_6 energy bands could be tuned by Mo-Mo and Mo-S bond length. It was reported that the bond length of intercluster Mo-Mo increased the most seriously while that of intercluster Mo-S increased the second most seriously with cation insertion.[42, 43] In contrast, the length of intracluster Mo-Mo and Mo-S bond changes only a little. Therefore, the intensity of peak A should be related to the intercluster Mo-Mo and/or intercluster Mo-S bond length. The disappearance of peak A for $Mg_2Mo_6S_8$ indicates at least one of the two bonding interactions is nearly extinct. Intercluster Mo-Mo bond is the only one that might be break as its bond length increases to 3.365 Å in $Mg_2Mo_6S_8$,[31] which is also supported by the insulating property of $Mg_2Mo_6S_8$.[23, 25] Thus we conclude intercluster Mo-Mo bond length, which mainly affects the hole number of specific Mo_6 bands, plays a key role in the intensity of peak A. The similar evolution can be seen with Li^+ inserted in Figure 5 (b). The decrease of peak A with one Li^+ inserted is contributed by the increase of intercluster Mo-Mo bond length while the disappearance results from the bond length increasing up to 3.408 Å.[13] Besides, the other pre-edge feature B is thought to be mainly related to the intracluster Mo-Mo and/or Mo-S bonds, where the slight changes of peak B is consistent with the little changes of intracluster bond length. Furthermore, as shown in Figure 4 (b), the intensity of peak A can be better related to the electrochemical reversibility than that of peak B. Therefore, it indicates that the electrochemical reversibility should be more closely related to intercluster Mo-Mo bonds than intracluster Mo-Mo bonds, which needs more detailed study in future.

CONCLUSIONS

We studied the charge distribution on S and intercluster bond evolution by comparing the XAS spectra of Mo_6S_8 with the insertion of cations in different types (i.e. Cu^+, Li^+ and Mg^{2+}) or in different amount. Pure Mo_6S_8 is proved to have a non-uniform charge distribution on S, which results from the difference in coordination number of Mo around S. The charge distribution on S becomes homogeneous with one cation inserted, which might result from the interaction between S_A and inserted cations. The electrochemical reversibility is found to correspond well to the reversible evolution of charge distribution. Given the correlation between chemical stability and charge distribution, the complete reversibility for Li storage indicates the electrochemical reversibility should be not only related to chemical stability. The evolution of certain Mo $L_{2,3}$ and S K pre-edge features with the insertion of different types of cations indicates that the deformation of Mo_6S_8 should result from the change of bond length induced by delocalization of inserted cations. This gives an experimental support to the "matrix effect". Further analysis indicates the intensity of peak A is mainly affected by intercluster Mo-Mo bond length. The electrochemical reversibility is demonstrated to be more closely related to intercluster Mo-Mo bond although the role and evolution of the bond need more detailed study. This study helps to clarify some fundamental debates and shed light on the mechanism of Mg storage in Mo_6S_8, which will inspire the development of Mg cathode material.

ASSOCIATED CONTENT

Supporting Information. This material is available free of charge via the Internet at http://pubs.acs.org.

Additional details about XRD pattern and SEM image of the as-prepared Mo_6S_8 and $CuMo_6S_8$, typical electrochemical test, XAS of Mo L3-edge and XANES of Mo K-edge.

AUTHOR INFORMATION

Corresponding Author

* E-mail: ypfaq@mail.sim.ac.cn and xliu3@mail.sim.ac.cn

Author Contributions

The manuscript was written through contributions of all authors. All authors have given approval to the final version of the manuscript.

Notes

The authors declare no competing financial interest.

ACKNOWLEDGMENT

The authors thank Fudong Han and Chunsheng Wang at University of Maryland for fruitful discussion on Mo_6S_8 synthesis and electrochemical experiments. The authors also thank Shih-Tien Tang, Ling-yun Jang and Ting-Shan Chan for helpful discussions about XAS experiment and analysis and synchrotron TLS for providing beamtime at the 16A beamline. This work was supported by the National Natural Science Foundation of China (Grant Nos. 21503263, U1632269, 21473235, and 11227902).

ABBREVIATIONS

VEC, valence electron concentration; BV, bond valence; XAS, X-ray absorption spectroscopy; Z_{eff}, effective nuclear charge, TLS, Taiwan light source; LUMO, lowest unoccupied molecular orbital.

REFERENCES

(1) Fischer, Ø., Chevrel phases: Superconducting and normal state properties. *Appl. Phys. A: Mater. Sci. Process.* **1978,** 16, (1), 1-28.

(2) Andersen, O. K.; Klose, W.; Nohl, H., Electronic structure of Chevrel-phase high-critical-field superconductors. *Phys. Rev. B* **1978,** 17, (3), 1209-1237.

(3) Hughbanks, T.; Hoffmann, R., Molybdenum chalcogenides: clusters, chains, and extended solids. The approach to bonding in three dimensions. *J. Am. Chem. Soc.* **1983,** 105, (5), 1150-1162.

(4) Johnson, D. C.; Tarascon, J. M.; Sienko, M. J., Structural and electronic instabilities in $M^{II}Mo_6S_8$ compounds. *Inorg. Chem.* **1985,** 24, (17), 2598-2604.

(5) King, R. B., Chemical bonding topology of superconductors: I. Ternary molybdenum chalcogenides (Chevrel phases). *J. Solid State Chem.* **1987,** 71, (1), 224-232.

(6) Imoto, H.; Saito, T.; Adachi, H., Molecular Orbital Calculations of Octahedral Molybdenum Cluster Complexes with the DV-X.alpha. Method. *Inorg. Chem.* **1995,** 34, (9), 2415-2422.

(7) Kobayashi, K.; Fujimori, A.; Ohtani, T.; Dasgupta, I.; Jepsen, O.; Andersen, O. K., Electronic structure of the Chevrel-phase compounds $Sn_xMo_6Se_{7.5}$: Photoemission spectroscopy and band-structure calculations. *Phys. Rev. B* **2001,** 63, (19), 195109.

(8) McKinnon, W. R.; Dahn, J. R., Structure and electrochemistry of $Li_xMo_6S_8$. *Phys. Rev. B* **1985,** 31, (5), 3084-3087.

(9) Dahn, J. R.; McKinnon, W. R.; Coleman, S. T., Lattice-parameter changes and triclinic distortions in $Li_xMo_6Se_8$ for 0<x<4. *Phys. Rev. B* **1985,** 31, (1), 484-489.

(10) Dahn, J. R.; McKinnon, W. R., Phase diagram of $Li_xMo_6Se_8$ for 0<x<1 from in situ x-ray studies. *Phys. Rev. B* **1985,** 32, (5), 3003-3005.

(11) Gocke, E.; Schoellhorn, R.; Aselmann, G.; Mueller-Warmuth, W., Molybdenum cluster chalcogenides Mo_6X_8: intercalation of lithium via electron/ion transfer. *Inorg. Chem.* **1987,** 26, (11), 1805-1812.

(12) Tarascon, J. M.; Hull, G. W.; Marsh, P.; Haar, T., Electrochemical, structural, and physical properties of the sodium Chevrel phases $Na_xMo_6X_{8-y}I_y$ (X = S, Se and y = 0 to 2). *J. Solid State Chem.* **1987,** 66, (2), 204-224.

(13) Ritter, C.; Gocke, E.; Fischer, C.; Schöllhorn, R., Neutron diffraction study on the crystal structure of lithium intercalated chevrel phases. *Mater. Res. Bull.* **1992,** 27, (10), 1217-1225.

(14) Fischer, C.; Gocke, E.; Stege, U.; Schöllhorn, R., Molybdenum Cluster Chalcogenides: In Situ X-Ray Studies on the Formation of $Cu_xMo_6S_8$ via Electron/Ion Transfer. *J. Solid State Chem.* **1993,** 102, (1), 54-68.

(15) Aurbach, D.; Lu, Z.; Schechter, A.; Gofer, Y.; Gizbar, H.; Turgeman, R.; Cohen, Y.; Moshkovich, M.; Levi, E., Prototype systems for rechargeable magnesium batteries. *Nature* **2000,** 407, 724.

(16) Lancry, E.; Levi, E.; Gofer, Y.; Levi, M.; Salitra, G.; Aurbach, D., Leaching Chemistry and the Performance of the Mo_6S_8 Cathodes in Rechargeable Mg Batteries. *Chem. Mater.* **2004,** 16, (14), 2832-2838.

(17) Lancry, E.; Levi, E.; Gofer, Y.; Levi, M. D.; Aurbach, D., The effect of milling on the performance of a Mo_6S_8 Chevrel phase as a cathode material for rechargeable Mg batteries. *J. Solid State Electrochem.* **2005,** 9, (5), 8.

(18) Levi, M. D.; Lancri, E.; Levi, E.; Gizbar, H.; Gofer, Y.; Aurbach, D., The effect of the anionic framework of Mo_6X_8 Chevrel Phase (X=S, Se) on the thermodynamics and the kinetics of the electrochemical insertion of Mg^{2+} ions. *Solid State Ionics* **2005,** 176, (19), 1695-1699.

(19) Mitelman, A.; Levi, M. D.; Lancry, E.; Levi, E.; Aurbach, D., New cathode materials for rechargeable Mg batteries: fast Mg ion transport and reversible copper extrusion in $Cu_yMo_6S_8$ compounds. *Chem. Commun.* **2007**, (41), 4212-4214.

(20) Woo, S.-G.; Yoo, J.-Y.; Cho, W.; Park, M.-S.; Kim, K. J.; Kim, J.-H.; Kim, J.-S.; Kim, Y.-J., Copper incorporated $Cu_xMo_6S_8$ ($x \geq 1$) Chevrel-phase cathode materials synthesized by chemical intercalation process for rechargeable magnesium batteries. *RSC Advances* **2014,** 4, (103), 59048-59055.

(21) Ichitsubo, T.; Yagi, S.; Nakamura, R.; Ichikawa, Y.; Okamoto, S.; Sugimura, K.; Kawaguchi, T.; Kitada, A.; Oishi, M.; Doi, T.; Matsubara, E., A new aspect of Chevrel compounds as positive electrodes for magnesium batteries. *Journal of Materials Chemistry A* **2014,** 2, (36), 14858-14866.

(22) Kganyago, K. R.; Ngoepe, P. E.; Catlow, C. R. A., Voltage profile, structural prediction, and electronic calculations for $Mg_xMo_6S_8$. *Phys. Rev. B* **2003,** 67, (10), 104103.

(23) Kaewmaraya, T.; Ramzan, M.; Osorio-Guillén, J. M.; Ahuja, R., Electronic structure and ionic diffusion of green battery cathode material: $Mg_2Mo_6S_8$. *Solid State Ionics* **2014,** 261, 17-20.

(24) Wan, L. F.; Perdue, B. R.; Apblett, C. A.; Prendergast, D., Mg Desolvation and Intercalation Mechanism at the Mo_6S_8 Chevrel Phase Surface. *Chem. Mater.* **2015,** 27, (17), 5932-5940.

(25) Thole, F.; Wan, L. F.; Prendergast, D., Re-examining the Chevrel phase Mo_6S_8 cathode for Mg intercalation from an electronic structure perspective. *Phys. Chem. Chem. Phys.* **2015,** 17, (35), 22548-22551.

(26) Rong, Z.; Malik, R.; Canepa, P.; Sai Gautam, G.; Liu, M.; Jain, A.; Persson, K.; Ceder, G., Materials Design Rules for Multivalent Ion Mobility in Intercalation Structures. *Chem. Mater.* **2015,** 27, (17), 6016-6021.

(27) Ling, C.; Suto, K., Thermodynamic Origin of Irreversible Magnesium Trapping in Chevrel Phase Mo_6S_8: Importance of Magnesium and Vacancy Ordering. *Chem. Mater.* **2017,** 29, (8), 3731-3739.

(28) Levi, M. D.; Lancry, E.; Gizbar, H.; Lu, Z.; Levi, E.; Gofer, Y.; Aurbach, D., Kinetic and Thermodynamic Studies of Mg^{2+} and Li^+ Ion Insertion into the Mo_6S_8 Chevrel Phase. *J. Electrochem. Soc.* **2004,** 151, (7), A1044-A1051.

(29) Levi, M. D.; Lancry, E.; Gizbar, H.; Gofer, Y.; Levi, E.; Aurbach, D., Phase transitions and diffusion kinetics during Mg^{2+} and Li^+ ion insertions into the Mo_6S_8 chevrel phase compound studied by PITT. *Electrochim. Acta* **2004,** 49, (19), 3201-3209.

(30) Levi, M. D.; Gizbar, H.; Lancry, E.; Gofer, Y.; Levi, E.; Aurbach, D., A comparative study of Mg^{2+} and Li^+ ion insertions into the Mo_6S_8 Chevrel phase using electrochemical impedance spectroscopy. *J. Electroanal. Chem.* **2004,** 569, (2), 211-223.

(31) Levi, E.; Lancry, E.; Mitelman, A.; Aurbach, D.; Ceder, G.; Morgan, D.; Isnard, O., Phase Diagram of Mg Insertion into Chevrel Phases, $Mg_xMo_6T_8$ (T = S, Se). 1. Crystal Structure of the Sulfides. *Chem. Mater.* **2006,** 18, (23), 5492-5503.

(32) Levi, E.; Mitelman, A.; Aurbach, D.; Brunelli, M., Structural Mechanism of the Phase Transitions in the Mg-Cu-Mo_6S_8 System Probed by ex Situ Synchrotron X-ray Diffraction. *Chem. Mater.* **2007,** 19, (21), 5131-5142.
(33) Levi, E.; Mitelman, A.; Aurbach, D.; Isnard, O., On the Mechanism of Triclinic Distortion in Chevrel Phase as Probed by In-Situ Neutron Diffraction. *Inorg. Chem.* **2007,** 46, (18), 7528-7535.
(34) Levi, E.; Gershinsky, G.; Aurbach, D.; Isnard, O.; Ceder, G., New Insight on the Unusually High Ionic Mobility in Chevrel Phases. *Chem. Mater.* **2009,** 21, (7), 1390-1399.
(35) Levi, E.; Levi, M. D.; Chasid, O.; Aurbach, D., A review on the problems of the solid state ions diffusion in cathodes for rechargeable Mg batteries. *Journal of Electroceramics* **2009,** 22, (1-3), 7.
(36) Levi, E.; Gershinsky, G.; Aurbach, D.; Isnard, O., Crystallography of Chevrel Phases, MMo_6T_8 (M = Cd, Na, Mn, and Zn, T = S, Se) and Their Cation Mobility. *Inorg. Chem.* **2009,** 48, (18), 8751-8758.
(37) Yvon, K.; Paoli, A., Charge transfer and valence electron concentration in Chevrel phases. *Solid State Commun.* **1977,** 24, (1), 41-45.
(38) Fischer, Ø.; Maple, M. B., *Superconductivity in Ternary Compounds I: Structural, Electronic, and Lattice Properties*. Springer, Berlin, Heidelberg: 1982; Vol. 32.
(39) Peña, O.; Sergent, M., Rare earth based chevrel phases $REMo_6X_8$: Crystal growth, physical and superconducting properties. *Prog. Solid State Chem.* **1989,** 19, (3), 165-281.
(40) Gocke, E.; Schramm, W.; Dolscheid, P.; Scho¨llhorn, R., Molybdenum cluster chalcogenides Mo_6X_8: Electrochemical intercalation of closed shell ions Zn^{2+}, Cd^{2+}, and Na^{+}. *J. Solid State Chem.* **1987,** 70, (1), 71-81.
(41) Corbett, J. D., Correlation of metal-metal bonding in halides and chalcides of the early transition elements with that in the metals. *J. Solid State Chem.* **1981,** 37, (3), 335-351.
(42) Levi, E.; Aurbach, D., Chevrel Phases, $M_xMo_6T_8$ (M = Metals, T = S, Se, Te) as a Structural Chameleon: Changes in the Rhombohedral Framework and Triclinic Distortion. *Chem. Mater.* **2010,** 22, (12), 3678-3692.
(43) Kubel, F.; Yvon, K., Matrix effect in chevrel phases containing divalent metal cations. The structure of rhombohedral $CaMo_6S_8$. *J. Solid State Chem.* **1988,** 73, (1), 188-191.
(44) Liu, X.; Liu, J.; Qiao, R.; Yu, Y.; Li, H.; Suo, L.; Hu, Y.-s.; Chuang, Y.-D.; Shu, G.; Chou, F.; Weng, T.-C.; Nordlund, D.; Sokaras, D.; Wang, Y. J.; Lin, H.; Barbiellini, B.; Bansil, A.; Song, X.; Liu, Z.; Yan, S.; Liu, G.; Qiao, S.; Richardson, T. J.; Prendergast, D.; Hussain, Z.; de Groot, F. M. F.; Yang, W., Phase Transformation and Lithiation Effect on Electronic Structure of Li_xFePO_4: An In-Depth Study by Soft X-ray and Simulations. *J. Am. Chem. Soc.* **2012,** 134, (33), 13708-13715.
(45) Liu, X.; Wang, D.; Liu, G.; Srinivasan, V.; Liu, Z.; Hussain, Z.; Yang, W., Distinct charge dynamics in battery electrodes revealed by in situ and operando soft X-ray spectroscopy. *Nat Commun* **2013,** 4, (1), 1-8.
(46) Liu, X.; Yang, W.; Liu, Z., Recent Progress on Synchrotron-Based In-Situ Soft X-ray Spectroscopy for Energy Materials. *Adv. Mater.* **2014,** 26, (46), 7710-7729.
(47) Liu, X.; Wang, Y. J.; Barbiellini, B.; Hafiz, H.; Basak, S.; Liu, J.; Richardson, T.; Shu, G.; Chou, F.; Weng, T.-C.; Nordlund, D.; Sokaras, D.; Moritz, B.; Devereaux, T. P.; Qiao, R.; Chuang, Y.-D.; Bansil, A.; Hussain, Z.; Yang, W., Why $LiFePO_4$ is a safe battery electrode: Coulomb repulsion induced electron-state reshuffling upon lithiation. *Phys. Chem. Chem. Phys.* **2015,** 17, (39), 26369-26377.
(48) Qiao, R.; Wray, L. A.; Kim, J.-H.; Pieczonka, N. P. W.; Harris, S. J.; Yang, W., Direct Experimental Probe of the Ni(II)/Ni(III)/Ni(IV) Redox Evolution in $LiNi_{0.5}Mn_{1.5}O_4$ Electrodes. *J. Phys. Chem. C.* **2015,** 119, (49), 27228-27233.
(49) Wang, L.; Song, J.; Qiao, R.; Wray, L. A.; Hossain, M. A.; Chuang, Y.-D.; Yang, W.; Lu, Y.; Evans, D.; Lee, J.-J.; Vail, S.; Zhao, X.; Nishijima, M.; Kakimoto, S.; Goodenough, J. B., Rhombohedral Prussian White as Cathode for Rechargeable Sodium-Ion Batteries. *J. Am. Chem. Soc.* **2015,** 137, (7), 2548-2554.
(50) Wan, L. F.; Wright, J.; Perdue, B. R.; Fister, T. T.; Kim, S.; Apblett, C. A.; Prendergast, D., Revealing electronic structure changes in Chevrel phase cathodes upon Mg insertion using X-ray absorption spectroscopy. *Phys. Chem. Chem. Phys.* **2016,** 18, (26), 17326-17329.
(51) Ravel, B.; Newville, M., ATHENA, ARTEMIS, HEPHAESTUS: data analysis for X-ray absorption spectroscopy using IFEFFIT. *Journal of Synchrotron Radiation* **2005,** 12, (4), 537-541.
(52) Groot, F. M. F. d.; Hu, Z. W.; Lopez, M. F.; Kaindl, G.; Guillot, F.; Tronc, M., Differences between L_3 and L_2 x-ray absorption spectra of transition metal compounds. *The Journal of Chemical Physics* **1994,** 101, (8), 6570-6576.
(53) de Groot, F. M. F., Differences between L_3 and L_2 X-ray absorption spectra. *Physica B: Condensed Matter* **1995,** 208, 15-18.
(54) Hedman, B.; Frank, P.; Gheller, S. F.; Roe, A. L.; Newton, W. E.; Hodgson, K. O., New structural insights into the iron-molybdenum cofactor from Azotobacter vinelandii nitrogenase through sulfur K and molybdenum L x-ray absorption edge studies. *J. Am. Chem. Soc.* **1988,** 110, (12), 3798-3805.
(55) Alperovich, I.; Smolentsev, G.; Moonshiram, D.; Jurss, J. W.; Concepcion, J. J.; Meyer, T. J.; Soldatov, A.; Pushkar, Y., Understanding the Electronic Structure of 4d Metal Complexes: From Molecular Spinors to L-Edge Spectra of a di-Ru Catalyst. *J. Am. Chem. Soc.* **2011,** 133, (39), 15786-15794.
(56) Sarangi, R.; Aboelella, N.; Fujisawa, K.; Tolman, W. B.; Hedman, B.; Hodgson, K. O.; Solomon, E. I., X-ray Absorption Edge Spectroscopy and Computational Studies on $LCuO_2$ Species: Superoxide−CuII versus Peroxide-CuIII Bonding. *J. Am. Chem. Soc.* **2006,** 128, (25), 8286-8296.
(57) Tenderholt, A. L.; Szilagyi, R. K.; Holm, R. H.; Hodgson, K. O.; Hedman, B.; Solomon, E. I., Electronic Control of the “Bailar Twist” in Formally d^0-d^2 Molybdenum Tris(dithiolene) Complexes: A Sulfur K-edge X-ray Absorption Spectroscopy and Density Functional Theory Study. *Inorg. Chem.* **2008,** 47, (14), 6382-6392.
(58) Rose Williams, K.; Hedman, B.; Hodgson, K. O.; Solomon, E. I., Ligand K-edge X-ray absorption spectroscopic studies: metal-ligand covalency in transition metal tetrathiolates. *Inorg. Chim. Acta* **1997,** 263, (1), 315-321.
(59) Szilagyi, R. K.; Lim, B. S.; Glaser, T.; Holm, R. H.; Hedman, B.; Hodgson, K. O.; Solomon, E. I., Description of the Ground State Wave Functions of Ni Dithiolenes Using Sulfur K-edge X-ray Absorption Spectroscopy. *J. Am. Chem. Soc.* **2003,** 125, (30), 9158-9169.
(60) Dey, A.; Chow, M.; Taniguchi, K.; Lugo-Mas, P.; Davin, S.; Maeda, M.; Kovacs, J. A.; Odaka, M.; Hodgson, K. O.; Hedman, B.; Solomon, E. I., Sulfur K-Edge XAS and DFT Calculations on Nitrile Hydratase: Geometric

and Electronic Structure of the Non-heme Iron Active Site. *J. Am. Chem. Soc.* **2006,** 128, (2), 533-541.

(61) Sarangi, R.; DeBeer George, S.; Rudd, D. J.; Szilagyi, R. K.; Ribas, X.; Rovira, C.; Almeida, M.; Hodgson, K. O.; Hedman, B.; Solomon, E. I., Sulfur K-Edge X-ray Absorption Spectroscopy as a Probe of Ligand-Metal Bond Covalency: Metal vs Ligand Oxidation in Copper and Nickel Dithiolene Complexes. *J. Am. Chem. Soc.* **2007,** 129, (8), 2316-2326.

(62) Hu, Z.; von Lips, H.; Golden, M. S.; Fink, J.; Kaindl, G.; de Groot, F. M. F.; Ebbinghaus, S.; Reller, A., Multiplet effects in the Ru $L_{2,3}$ x-ray-absorption spectra of Ru(IV) and Ru(V) compounds. *Phys. Rev. B* **2000,** 61, (8), 5262-5266.

(63) Shadle, S. E.; Hedman, B.; Hodgson, K. O.; Solomon, E. I., Ligand K-Edge X-ray Absorption Spectroscopy as a Probe of Ligand-Metal Bonding: Charge Donation and Covalency in Copper-Chloride Systems. *Inorg. Chem.* **1994,** 33, (19), 4235-4244.

(64) Weber, T.; Muijsers, J. C.; Niemantsverdriet, J. W., Structure of Amorphous MoS_3. *The Journal of Physical Chemistry* **1995,** 99, (22), 9194-9200.

(65) Hibble, S. J.; Rice, D. A.; Pickup, D. M.; Beer, M. P., Mo K-edge EXAFS and S K-edge absorption studies of the amorphous molybdenum sulfides $MoS_{4.7}$, MoS_3, and MoS_3•nH2O (n~2). *Inorg. Chem.* **1995,** 34, (21), 5109-5113.

(66) Brese, N. E.; O'Keeffe, M., Bond-valence parameters for solids. *Acta Crystallographica Section B* **1991,** 47, (2), 192-197.

(67) Sarangi, R.; DeBeer George, S.; Rudd, D. J.; Szilagyi, R. K.; Ribas, X.; Rovira, C.; Almeida, M.; Hodgson, K. O.; Hedman, B.; Solomon, E. I., Sulfur K-Edge X-ray Absorption Spectroscopy as a Probe of Ligand−Metal Bond Covalency: Metal vs Ligand Oxidation in Copper and Nickel Dithiolene Complexes. *J. Am. Chem. Soc.* **2007,** 129, (8), 2316-2326.

For Table of Contents Only